



June 2007

Glass formation of ternary Sm-based Sm-Al-Co bulk metallic glasses

Jiang Wu

State Key Lab of Materials Modification, Dalian University of Technology, Dalian 116024, China

Qing Wang

State Key Lab of Materials Modification, Dalian University of Technology, Dalian 116024, China

Weirong Chen

State Key Lab of Materials Modification, Dalian University of Technology, Dalian 116024, China

Qingyu Zhang

State Key Lab of Materials Modification, Dalian University of Technology, Dalian 116024, China

Jianbing Qiang

State Key Lab of Materials Modification, Dalian University of Technology, Dalian 116024, China

See next page for additional authors

Follow this and additional works at: <https://ustb.researchcommons.org/ijmmm>

Recommended Citation

Wu Jiang, Wang Qing, Chen Weirong, Zhang Qingyu, Qiang Jianbing, Dong Chuang. Glass formation of ternary Sm-based Sm-Al-Co bulk metallic glasses, *Int. J. Miner. Metall. Mater.*, 14 (2007), No. 7, Article 12, p. 50-53.

This Research is brought to you for free and open access by International Journal of Minerals, Metallurgy and Materials. It has been accepted for inclusion in International Journal of Minerals, Metallurgy and Materials by an authorized editor of International Journal of Minerals, Metallurgy and Materials.

Glass formation of ternary Sm-based Sm-Al-Co bulk metallic glasses

Authors

Jiang Wu, Qing Wang, Weirong Chen, Qingyu Zhang, Jianbing Qiang, and Chuang Dong

Glass formation of ternary Sm-based Sm-Al-Co bulk metallic glasses

Jiang Wu¹⁾, Qing Wang¹⁾, Weirong Chen¹⁾, Qingyu Zhang¹⁾, Jianbing Qiang¹⁾, and Chuang Dong^{1,2)}

1) State Key Lab of Materials Modification, Dalian University of Technology, Dalian 116024, China

2) International Center of Materials Physics, Chinese Academy of Sciences, Shenyang, 110016, China

(Received 2006-06-20)

Abstract: Ternary Sm-based Sm-Al-Co alloys at specific compositions designed using an e/a - and cluster-related criteria exhibit high glass forming abilities and form bulk glassy rods of 3 mm in diameter by a copper mold suction-casting method. Four compositions of bulk metallic glasses (BMGs) are $\text{Sm}_{50}\text{Al}_{25}\text{Co}_{25}$, $\text{Sm}_{52}\text{Al}_{24}\text{Co}_{24}$, $\text{Sm}_{54}\text{Al}_{23}\text{Co}_{23}$ and $\text{Sm}_{56}\text{Al}_{22}\text{Co}_{22}$, which all satisfy a constant conduction electron concentration of 1.5. Among them, the BMG exhibiting the largest reduced glass transition temperature (T_{rg}) is $\text{Sm}_{50}\text{Al}_{25}\text{Co}_{25}$, which reaches 0.648. The glass transition temperature T_g and the onset crystallization temperature T_x of this alloy are respectively 579 and 640 K at a heating rate of 20 K/min.

Key words: Sm-based alloys; bulk metallic glasses; alloy design; cluster line; electron concentration

[This work was financially supported by the National Natural Science Foundation of China (No.50401020, 50671018 and 50631010) and the Provincial Science and Technology Foundation of Liaoning (No.20061067).]

1. Introduction

In the last decade, great progress has been achieved in the research of rare earth (RE) metal-based bulk metallic glasses. The casting size of La-based bulk metallic glasses (BMGs) has increased to more than 10 mm using the conventional copper mould casting method [1]. Rods of Nd-based BMGs reached 12 mm in diameter, and some of them displayed good hard magnetic properties [2]. On the other hand, many new families of RE-based BMGs have been discovered, such as Pr- [3], Ce- [4], Gd- [5], Dy- [6], Ho- [7], and Sm-based [8-10]. These alloys usually exhibit good glass forming ability (GFA) and have potential industrial applications [3-11]. For example, the new Ce-based BMG with a low T_g (glass transition temperature) close to room temperature attracts much attention due to its polymer-like thermoplastic behavior [11]. For the Sm-based alloy systems, its GFA has still not been investigated extensively. The first Sm-based BMG is a $\text{Sm}_{60}\text{Fe}_{10}\text{Al}_{10}\text{Co}_{15}\text{Cu}_5$ quinary alloy prepared by die casting, which shows a ferromagnetic behavior [8]. The second Sm-based BMG is a Sm-Al-Ni-Cu quaternary system [9]. Recently, several ternary Sm-Al-Ni BMGs with a diameter of 3 mm have been discovered by our group [10]. However, the glass formation for other Sm-based BMG systems is still un-

known, especially for the Sm-Co-based alloys which are promising for applications as magnetic materials because the family of Sm-Co alloys or compounds are excellent permanent-magnetic materials [12].

In this paper, a new series of ternary Sm-Al-Co BMGs was reported. Their composition optimization was accomplished by using the e/a - and cluster-based criteria. A ternary cluster was used as the cluster criterion, which is an extension of the present binary cluster-based criterion.

2. Composition design

The structural stability in relation to the conduction electron concentration per atom (e/a) has been revealed to be a universal feature of many electronically simple and transition metal-containing alloys. The e/a values of BMGs and their related crystalline phases are nearly constant. The e/a -constant feature is represented in a ternary phase diagram by a straight composition line with a constant e/a value. The optimized BMGs and their crystalline counterparts are located along this line. Such an e/a -constant criterion has been applied in the composition optimization of many Zr-based systems such as Zr-Al-(Ni,Co,Cu) [13-15] and the Sm-based Sm-Al-Ni system [10].

The effective e/a value of Sm must be determined

before this criterion can be used. Due to the predominant Brillouin Zones (BZs) corresponding to the most intense diffraction peaks, the most intense peak can be used to calculate the BZ width $K_p=4\pi\sin\theta_p/\lambda$, where θ_p is the diffraction angle of the intense diffuse peaks in the XRD pattern and λ is the X-ray wavelength. Wang *et al.* have calculated $(e/a)_{Zr}=1.5$ [15], associating this diffraction method with the formulation of $2K_f\approx K_p$ that denotes the BMG stabilization mechanism, where K_f is the Fermi wave vector [16]. The rare-earth metal Sm is considered as its crystalline form hP-Sm, which exhibits the most intense diffraction peak (004) at $\theta_p=15.24^\circ$ when the multiplicity factor is considered. This relationship gives $K_p=21.45\text{ nm}^{-1}$. When the $2K_f\approx K_p$ rule is satisfied, $K_f=10.72\text{ nm}^{-1}$. The conduction electron concentration per unit volume N_v is 41.633 nm^{-3} using $K_f=(3\pi^2N_v)^{1/3}$. Finally, since $N_v=(e/a)\rho$, where ρ is the atom number per volume and can be calculated by the atom number (4) and the volume (0.1326 nm^{-3}) of the unit cell, the effective e/a of Sm is obtained, about 1.4, which is very close to that of the metal Zr 1.43. Considering a small charge transfer between alloying elements, the e/a of Zr is finally 1.5 in Zr-based BMGs [15] and related crystalline phases. Similarly, the e/a of Sm is approximately taken as 1.5 in this alloys. Thus, in the Sm-Al-Co ternary system, two known phases, AlCo (cP-CsCl type) and pure Sm fall along a straight composition line with $e/a=1.5$, where the electron concentration contributions from Al and Co are 3 and 0 respectively [13-14].

The second criterion is the cluster line criterion, which refers to a characteristic composition line in a ternary composition chart, linking a specific cluster composition point of a binary subsystem with high GFA, usually near a deep eutectic composition, to the third constituent. This line has been widely applied in our previous studies on the composition optimization of the Zr- or Cu-based ternary systems [13,17]. Therefore, the cluster line combines the binary clusters with the optimum glass forming compositions in a given ternary alloy system. The key step in our composition design is to select appropriate clusters for cluster lines. In the previous composition optimization in the Zr- or Cu-based ternary systems, the icosahedral clusters were used [13,17-18]. However, ternary clusters have not been considered to define cluster lines.

Icosahedral short-range ordering dominates in many amorphous alloy structures [19]. Experimental evidence indicated that the existence of the icosahedral atomic clusters in the amorphous structures contributes to the high glass forming ability and the high stability against crystallization [20]. Thus, in the current work, an icosahedron Sm_8AlCo_4 was used to con-

struct the cluster line. This icosahedral cluster is derived from the $\text{Al}_7\text{Co}_6\text{Sm}_6$ phase and centered by an Al atom. In addition, according to Miracle's topologically effective atomic packing model [21], the ratio R between the radius r_0 of the center atom and the average radius r_1 of the nearest-neighbor shell atoms for the Sm_8AlCo_4 cluster was calculated. The value of R is found to be 0.885, which is very close to the ideal $R^*=0.902$, under the condition of efficient atomic packing for the same coordination number of the nearest-neighbor shell cluster. The difference between R and R^* is only 1.9%, which indicates that the Sm_8AlCo_4 cluster satisfies topologically effective atomic packing. Furthermore, the element Al was used to construct the cluster line $(\text{Sm}_7\text{Ni}_3)\text{-Al}$ in the Sm-Al-Ni system [10]. Similarly, in the Sm-Al-Co system, the cluster line $(\text{Sm}_8\text{AlCo}_4)\text{-Al}$ was constructed by extending a line from the Sm_8AlCo_4 icosahedral cluster to the element Al.

Two composition lines are constructed in the Sm-based Sm-Al-Co system, one being the e/a -constant line $(\text{AlCo})\text{-Sm}$ with $e/a=1.5$, and the second cluster composition line $(\text{Sm}_8\text{AlCo}_4)\text{-Al}$, as shown in Fig. 1. The intersecting point of the two lines is $\text{Sm}_{50}\text{Al}_{25}\text{Co}_{25}$. To confirm the glass-forming range near this intersection, six alloy compositions from $\text{Sm}_{48}\text{Al}_{24}\text{Co}_{24}$ to $\text{Sm}_{58}\text{Al}_{21}\text{Co}_{21}$ along the $e/a=1.5$ line have been studied.

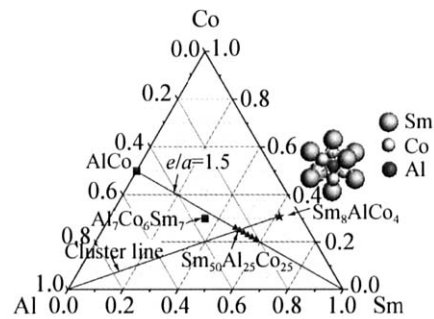


Fig. 1. Bulk metallic glass composition chart in the Sm-Al-Co system.

3. Experimental

Six ingots of compositions $\text{Sm}_{48}\text{Al}_{26}\text{Co}_{26}$, $\text{Sm}_{50}\text{Al}_{25}\text{Co}_{25}$, $\text{Sm}_{52}\text{Al}_{24}\text{Co}_{24}$, $\text{Sm}_{54}\text{Al}_{23}\text{Co}_{23}$, $\text{Sm}_{56}\text{Al}_{22}\text{Co}_{22}$, and $\text{Sm}_{58}\text{Al}_{21}\text{Co}_{21}$ were prepared by arc melting the mixtures of constituent elements under an argon atmosphere. The purities of elements are 99.9wt% for Sm, 99.999wt% for Al and 99.99wt% for Co, respectively. A small excess of Sm was added to compensate for mass loss due to evaporation during melting. Alloy rods with a diameter of 3 mm were prepared by means of copper mould suction casting. Structural identification of these alloys was carried out

by means of X-ray diffractometry (XRD) on the bottom end of the rods using Cu K_{α} radiation ($\lambda=0.15406$ nm). High-resolution transmission electron microscopy (HRTEM) was carried out on a Tecnai G² 20 for the crushed BMG powder samples. Differential Scanning Calorimetry (DSC) was done on a TA Q100 at a heating rate of 20 K/min.

4. Results and discussion

Fig. 2 shows the XRD patterns for the six as-cast rods. The broad diffused diffraction peaks in the patterns indicate that BMGs are formed in a very narrow range along the $e/a=1.5$ line. Only four alloys $\text{Sm}_{50}\text{Al}_{25}\text{Co}_{25}$, $\text{Sm}_{52}\text{Al}_{24}\text{Co}_{24}$, $\text{Sm}_{54}\text{Al}_{23}\text{Co}_{23}$, and $\text{Sm}_{56}\text{Al}_{22}\text{Co}_{22}$ among the six alloys form pure BMG rods. The amorphous nature of these samples is further confirmed by HRTEM. Fig. 3 presents a high-resolution image and a selected-area electron diffraction pattern for the as-cast sample $\text{Sm}_{50}\text{Al}_{25}\text{Co}_{25}$, showing a pure single amorphous phase without evident nanocrystals.

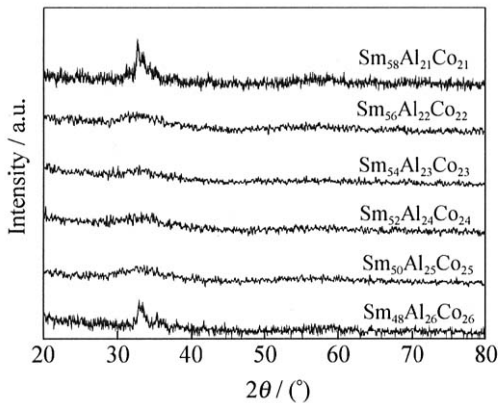


Fig. 2. XRD patterns of alloys lying on the $e/a = 1.5$ line.

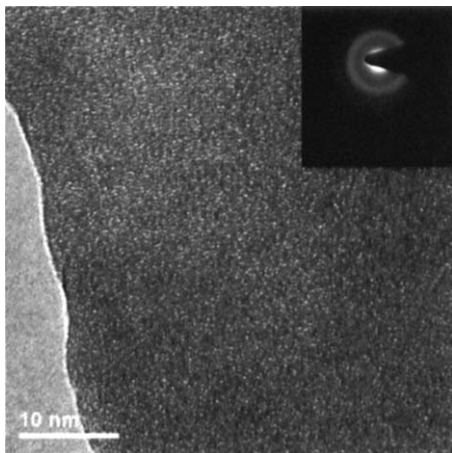


Fig. 3. Selected-area electron diffraction pattern and high-resolution image of the $\text{Sm}_{50}\text{Al}_{25}\text{Co}_{25}$ BMG.

The DSC traces of the four BMG forming samples are shown in Fig. 4. All the traces exhibit an obvious glass transition, a crystallization exothermic peak, and

an endothermic signal corresponding to the melting process.

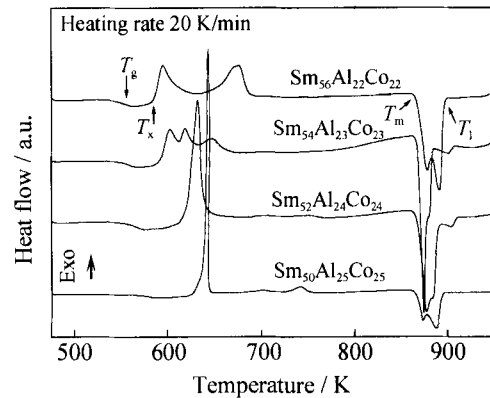


Fig. 4. DSC traces of the BMGs on the 1.5 e/a -constant line.

The characteristic thermodynamic temperatures of these BMGs are listed in Table 1, including the glass transition temperature (T_g), the onset temperature of crystallization (T_x), the onset temperature of melting (T_m), the offset melting point (T_l), the supercooled liquid region ΔT_x ($\Delta T_x=T_x-T_g$) and GFA indicators, such as the reduced glass transition temperature T_{rg} ($T_{rg}=T_g/T_l$ [22]) and γ ($\gamma=T_x/(T_g+T_l)$ [23]) of the BMGs.

Among the characteristic data, T_g and T_x are indices of the thermal stability of a glassy alloy. High T_g and T_x signify high resistance against crystallization. As can be seen from Table 1, both T_g and T_x of these BMGs are strongly dependent on the alloy compositions, and decrease with increasing Sm contents. ΔT_x can serve as another index for the thermal stability of the supercooled liquid. ΔT_x has the similar tendency to T_g and T_x with respect to the BMG compositions in this study. Among these four BMGs, the $\text{Sm}_{50}\text{Al}_{25}\text{Co}_{25}$ alloy displays the highest thermal stability with the largest value of T_g (579 K), T_x (640 K) and ΔT_x (61 K).

The reduced glass transition temperature T_{rg} ($T_{rg}=T_g/T_m$ or T_g/T_l) is generally accepted as the foremost GFA parameter. According to Lu *et al.* [22], T_g/T_l is more linked to GFA than T_g/T_m . Therefore, $T_{rg}=T_g/T_l$ are used to estimate the GFA of an amorphous alloy in this paper. The γ parameter, $\gamma=T_x/(T_g+T_l)$, is also used as a measure of GFA. A good GFA is associated with $T_{rg}\geq 0.6$ and $\gamma\geq 0.35$ [11]. The values of T_g/T_l and γ in Table 1 are all larger than 0.6 and 0.35, respectively, which means that these four BMGs have large GFAs. It is also noted that the values of T_g/T_l and γ show the same tendency as T_g and T_x , *i.e.* decreasing with increasing Sm contents, and that the GFA in this system is strongly sensitive to the compositions. The best GFA appears in the $\text{Sm}_{50}\text{Al}_{25}\text{Co}_{25}$ BMG with the largest T_g/T_l (0.648) and γ (0.435). This composition is

located at the intersection of the e/a -constant line with $e/a = 1.5$ and the cluster composition line (Sm_8AlCo_4)-Al.

Table 1. Characteristic thermodynamic temperatures of these BMGs

Composition	T_g / K	T_x / K	T_m / K	T_l / K	$\Delta T_x / \text{K}$	T_g/T_l	γ
$\text{Sm}_{50}\text{Al}_{25}\text{Co}_{25}$	579	640	867	893	61	0.648	0.435
$\text{Sm}_{52}\text{Al}_{24}\text{Co}_{24}$	566	621	868	910	55	0.622	0.421
$\text{Sm}_{54}\text{Al}_{23}\text{Co}_{23}$	557	592	868	906	35	0.615	0.405
$\text{Sm}_{56}\text{Al}_{22}\text{Co}_{22}$	554	585	868	895	31	0.619	0.404

Therefore, the optimum $\text{Sm}_{50}\text{Al}_{25}\text{Co}_{25}$ BMG, with both the highest thermal stability and largest GFA in the investigated Sm-Al-Co alloys, is located at the intersection of the e/a -constant line with $e/a = 1.5$ and the cluster composition line of (Sm_8AlCo_4)-Al. The characteristic parameters of this BMG are $T_g=579$ K, $T_x=640$ K, $T_g/T_l=0.648$ and $\gamma=0.435$, respectively. This is very similar to that in the Zr-Al-Ni system [14] and the Sm-Al-Ni system [10].

5. Conclusions

The application of our e/a - and cluster-based criteria in the Sm-Al-Co system has led to the discovery of novel ternary Sm-based BMGs. The $\text{Sm}_{50}\text{Al}_{25}\text{Co}_{25}$ BMG, located at the intersection point of the cluster line (Sm_8AlCo_4)-Al and the e/a -constant line, has the best thermal stability and glass forming ability, characterized by $T_g=579$ K, $T_x=640$ K, $T_g/T_l=0.648$ and $\gamma=0.435$.

References

- [1] Y. Zhang, H. Tan, and Y. Li, Bulk glass formation of 12 mm rod in La-Cu-Ni-Al alloys, *Mater. Sci. Eng. A*, 375-77(2004), p.436.
- [2] A. Inoue, T. Zhang, A. Takeuchi, et al., Hard magnetic bulk amorphous Nd-Fe-Al alloys of 12 mm in diameter made by suction casting, *Mater. Trans. JIM*, 37(1996), p.636.
- [3] A. Inoue, T. Zhang, and A. Takeuchi, Preparation of bulk Pr-Fe-Al amorphous alloys and characterization of their hard magnetic properties, *Mater. Trans. JIM*, 37(1996), p.1731.
- [4] B. Zhang, D.Q. Zhao, M.X. Pan, et al., Formation of cerium-based bulk metallic glasses, *Acta Mater.*, 54(2006), p.3025.
- [5] S. Li, R.J. Wang, M.X. Pan, et al., Heavy rare earth based bulk metallic glasses with high thermal stability, *Intermetallics*, 14(2006), p.592.
- [6] S. Li, R.J. Wang, M.X. Pan, et al., Bulk metallic glasses based on heavy rare earth dysprosium, *Scripta Mater.*, 53(2005), p.1489.
- [7] Q. Luo, D.Q. Zhao, M.X. Pan, et al., Hard and fragile holmium-based bulk metallic glasses, *Appl. Phys. Lett.*, 88(2006), p.181909.
- [8] G.J. Fan, W. Loser, S. Roth, et al., Glass-forming ability of RE-Al-TM alloys (RE=Sm, Y; TM=Fe, Co, Cu), *Acta Mater.*, 48(2000), p.3823.
- [9] Y.Q. Wang, J. Li, R. Tian, et al., Bulk metallic glasses in Sm-Cu-Ni-Al alloy systems, *J. Rare Earth*, 23(2005), p.415.
- [10] J. Wu, Q. Wang, J.B. Qiang, et al., Sm-based Sm-Al-Ni ternary bulk metallic glasses, *J. Mater. Res.*, 22(2007), p.573.
- [11] B. Zhao, D.Q. Zhao, M.X. Pan, et al., Amorphous metallic plastic, *Phys. Rev. Lett.*, 94(2005), p.205502.
- [12] K.H.J. Buschow, Intermetallic compounds of rare-earth and 3d transition metals, *Rep. Prog. Phys.*, 40(1977), p.1179.
- [13] Y.M. Wang, X.F. Zhang, J.B. Qiang, et al., Composition optimization of the Al-Co-Zr bulk metallic glasses, *Scripta Mater.*, 50(2004), p.829.
- [14] Y.M. Wang, C.H. Shek, J.B. Qiang, et al., The e/a criterion for the largest glass-forming abilities of the Zr-Al-Ni(Co) alloys, *Mater. Trans. JIM*, 45(2004), p.1180.
- [15] Y.M. Wang, W.P. Xu, J.B. Qiang, et al., The e/a criterion of Zr-based bulk metallic glasses, *Mater. Sci. Eng. A*, 375-377(2004), p.411.
- [16] S.R. Nagel and J. Tauc, Nearly-free-electron approach to the theory of metallic glass alloys, *Phys. Rev. Lett.*, 35(1975), p.380.
- [17] Q. Wang, J.B. Qiang, Y.M. Wang, et al., Formation and optimization of Cu-based Cu-Zr-Al bulk metallic glasses, *Mater. Sci. Forum*, 475-479(2005), p.3381.
- [18] J.H. Xia, J.B. Qiang, Y.M. Wang, et al., Ternary bulk metallic glasses formed by minor alloying of Cu₈Zr₅ icosahedron, *Appl. Phys. Lett.*, 88(2006), p.101907.
- [19] L.C. Chen and F. Spaepen, Calorimetric evidence for the microquasicrystalline structure of amorphous Al/transition metal alloys, *Nature*, 336(1988), p.366.
- [20] J. Saida, M. Matsushita, C. Li, et al., Effects of Ag and Pd on the nucleation and growth of the nano-icosahedral phase in $\text{Zr}_{65}\text{Al}_{7.5}\text{Ni}_{10}\text{Cu}_{7.5}\text{M}_{10}$ (M=Ag or Pd) metallic glasses, *Philos. Mag. Lett.*, 80(2000), p.737.
- [21] D.B. Miracle, W.S. Sanders, and O.N. Senkov, The influence of efficient atomic packing on the constitution of metallic glasses, *Philos. Mag.*, 83(2003), p.2409.
- [22] Z.P. Lu, H. Tan, Y. Li, et al., Correlation between reduced glass transition temperature and glass forming ability of bulk metallic glasses, *Scripta Mater.*, 42(2000), p.667.
- [23] Z.P. Lu and C.T. Liu, A new glass-forming ability criterion for bulk metallic glasses, *Acta Mater.*, 50(2002), p.3501.